The Gálvez-Davison Index for Tropical Convection

Preliminary Draft, 10 September 2015

JOSE M. GALVEZ
Systems Research Group, College Park, Maryland

MICHEL DAVISON
NOAA/NWS/NCEP Weather Prediction Center, College Park, Maryland

ABSTRACT

The Gálvez-Davison Index (GDI) is a stability index developed to improve the prediction of thunderstorms and shallower types of moist convection in the tropics. The motivation was the need of a skillful index to forecast tropical convection, particularly in the Caribbean, where traditional stability indices struggle as they were designed with extra tropical latitudes in mind.

The GDI focuses on thermodynamic properties of the low and mid troposphere. It is calculated from temperatures and mixing ratios available at 500, 700, 850 and 950 hPa. It can therefore be easily computed from radiosonde data, other analyses or model data. The GDI considers three physical processes that modulate tropical convection: (1) the simultaneous availability of heat and moisture in the mid and low troposphere, (2) the stabilizing/destabilizing effects of a warmer/cooler mid troposphere in association with ridges/troughs and (3) the entrainment of dry air and stabilization associated with subsidence inversions.

Validation over the Tropical and Subtropical Americas shows the GDI frequently outperforming most traditional stability indices in the diagnosis of the potential for different regimes of moist convection. It further proved useful in the prediction of extra tropical warm season air mass thunderstorms outperforming even the K index, the index of choice for tropical convection. The GDI performs best in trade-wind regime climates and regions downwind. This is especially true across the northern Caribbean-Mexico and Southeastern Brazil. In these locations, the GDI explains as much as >50% and >70% of the variances of brightness temperature and outgoing long wave radiation respectively when data is inter-compared using a 2°x2° grid.

1. Introduction

Stability indices are quantities designed to evaluate the potential for different types of convection and to be readily computed from sounding data (Glickman, 2000). They are important tools for weather forecasters as they provide a prompt but comprehensive analysis of the static stability of the atmosphere, which reduces the amount of time required to evaluate the potential for convection. The stability indices have been developed and used routinely since the 1940s. A brief description of traditional stability indices that are still commonly used to forecast convection is provided in Table 1.

There are several other quantities considered as efficient parameters for forecasting moist convection. Two quantities largely used are the Convective Available Potential Energy (CAPE) and the Convective Inhibition (CIN). CAPE describes the energy available for moist convection in an air column once a parcel is lifted to the level of free convection, where it becomes buoyant with respect to its environment. It is often used together with CIN, which describes the energy that a parcel needs to overcome the capping inversion during ascent and become buoyant (Moncrieff and Miller, 1976; Doswell and Rasmussen, 1994; Blanchard, 1998). Other indices related to moist convection exist, but their main focus relies on other aspects of it such as severity, e.g., the SWEAT index (Miller, 1972). A comprehensive description of several indices used for thunderstorms forecasting can be found in Harklander and Van Delden (2003).

Table 1. Traditional Stability Indices that are still actively used to forecast moist convection.

Index	Reference	Summary
Showalter	Showalter (1947)	Estimates convective instability by comparing the difference between the 500 hPa temperature and that of a parcel rising from 850 hPa following the dry adiabat until saturated, and then the moist adiabat.
K	George (1960)	The K index was developed for forecasting air mass thunderstorms. It considers an 850-500hPa lapse rate term and an 850-700 hPa moisture term. Since it considers moisture up to the 700 hPa level, it often outperforms most indices in the tropics where stability is largely sensitive to mid-tropospheric moisture. Although very helpful, its performance over mountainous terrain is limited.
Lifted	Galway (1966)	Similar to the Showalter index but the parcel is lifted from the boundary layer top. Although methods for the determination of this height vary, it is often determined using the warmest diurnal temperature and the mean mixing ratio at 2m, predicted if necessary. This height often falls within the lowest 900m of the profile and Lifted Index values tend to be lower than those of the Showalter index.
Total Totals	Miller (1967)	It is based upon an 850-500hPa lapse rate term and upon an cross moisture-temperature term that is largely sensitive to 850 hPa moisture. It was designed for applications in the United States (Peppler and Lamb, 1989).

Stability has a major role on the development of moist convection but this role differs between the tropics and the extra tropics. While in the latter perturbations are often dynamically robust and easily capable of triggering convection, tropical perturbations tend to be dynamically weak and convection is left to largely rely on column stability. The processes that drive convection also differ between the tropics and the extra tropics. This combination of factors leads to skill limitations when traditional stability indices that were developed for the extra tropics are used to forecast tropical convection (Schultz, 1989; Jacovides and Yonetani, 1990; Huntrieser et al., 1997; Harklander and Van Delden, 2003). This is illustrated in Fig. 1.

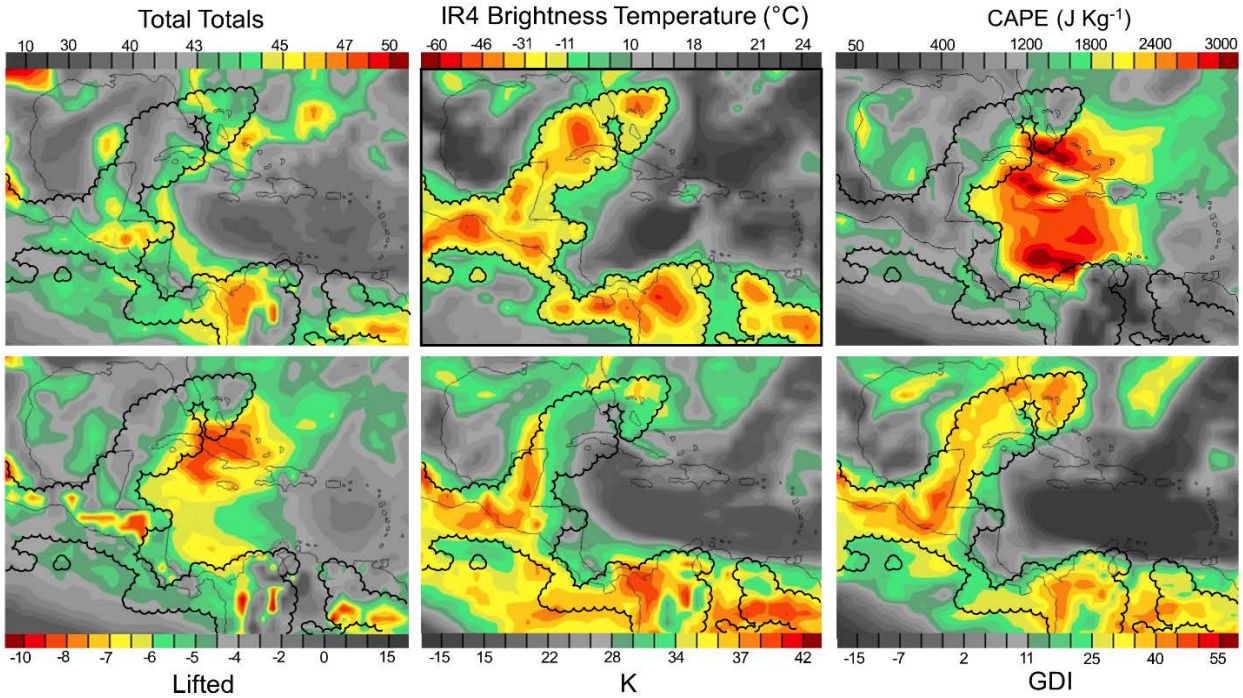

Figure 1. Intercomparison of GOES IR4-derived brightness temperatures (top center) against five stability indices computed from GFS F00-F12 data (remaining panels). All fields are averaged over 12 hours during 00Z-12Z 16 August 2013. The indices presented include the total totals (top left), CAPE (top right), Lifted (bottom left), K (bottom center) and the newly developed Gálvez-Davison Index GDI (bottom right). The outline corresponding to cloud tops colder than -10°C is overlaid in all panels.

Figure 1 is an example of the performance of four traditional indices/quantities as predictors for deep convection during a Caribbean/Central American rainy season evening. Enhanced convection is interpreted as low brightness temperature averages produced by persistent cold cloud tops. Some cirrus contamination was present but to a limited extent. The distribution of convection is compared against GFS-calculated index values using black curly outlines. These encircle the areas where cold tops persisted long enough to produce temperature averages below -10°C. Discrepancies between the distribution of index values and convection are evident, and although the comparison was made over a 12-hour period, this example represents repeatedly encountered index skill limitations on the prediction of tropical convection and corresponding coverage.

Figure 1 also illustrates that the K index was the most skillful compared to the Total Totals, CAPE and Lifted, a commonly encountered outcome. This skill arises from the consideration of 700hPa moisture, a quantity closely related to buoyancy in the tropical mid troposphere (Caesar, 2005), which makes the K index of choice in the prediction of tropical convection. But even the K has limitations. It exhibits low variability in shallow convection regimes, particularly in equatorial latitudes; and disregards thermodynamic properties below 850 hPa. Layers closer to the surface do matter to determine column stability in the tropics as the spatial and temporal distributions of heat and moisture can sometimes vary significantly. Such skill limitations affect the prediction of tropical convection which is an issue encountered on a daily basis on weather forecasting practices conducted at the Weather Prediction Center (WPC) International Desks as well as by the meteorologists of the national meteorological centers in the Caribbean basin and Latin America.

The necessity of a skillful index for the prediction of tropical convection motivated the WPC International Desks to dedicate efforts into the development of the Gálvez-Davison Index (GDI). The GDI was developed based on physical processes that dominate the variability of tropical convection with special emphasis on trade wind convection. Validation results are encouraging. They show that the GDI often outperforms most indices, even the K, as exemplified on Figure 1. Validation results also show remarkable GDI performance in the subtropics and even extra tropics during warm season convective events. This manuscript elaborates on the philosophy behind the GDI, presents the calculation algorithm and discusses GDI performance and applicability upon validation exercises conducted over the Americas.

2. Background

The evaluation of stability in an air column is an essential initial step in the process of forecasting moist convection, and this is especially true in the tropics. Stability/instability can be regarded as a measure of the reluctance/readiness of an atmospheric layer to produce convective overturning when slightly disturbed. The forecast of convection thus relies on the detection of potential interactions between perturbations and weakly stable layers. The strength and size of perturbations matters, and this differs among the tropics and the extra tropics. Extra tropical perturbations are often substantial in size and strength due to enhanced baroclinicity and associated strong winds. Large scale dynamics commonly play a strong role on the generation of extra tropical convection, even in environments where some degree of stability is present. This is rarely the case in the tropics where perturbations are generally weak. Regions of ascent are accordingly weak and occur in smaller scales, as they are predominantly driven by surface heat fluxes and infrared radiation (Neelin and Held, 1987; Raymond 2000a), processes that are tied to the local geography and convection itself (Randall and Huffman, 1980; Grabowski and Moncrieff, 2004). The shortage of robust perturbations that trigger tropical convection largely heightens its sensitivity to column stability.

Column stability and associated convection are also driven by different mechanisms in the tropics than in the extra tropics. One characteristic of tropical convection is its enhanced sensitivity to moisture content. Weak stability is a regular feature in the tropical troposphere, and in such environments moisture

availability largely matters due to its modulation of air parcel buoyancy. Once convection initiates in a moist tropical environment the limited amount of dry air entrainment results in a rapid release of latent heat. The warming produced destabilizes the column and convective development is expedited. Moist tropical environments thus favor the setup of a positive feedback mechanism that favors convection maintenance once initiation occurs. The developing convection also results on a water vapor increase in the free troposphere due to cloud detrainment and evaporation from precipitation. This moistening destabilizes the column facilitating future convective development in nearby and downwind locations. This process is the basis for the Moisture-Convection Feedback described by Grabowski and Moncrieff (2004), which shows that the potential for the development of tropical convection is largely conditioned by the occurrence of foregoing convection (Randall and Huffman, 1980; Grabowski and Moncrieff, 2004), and this is a key concept behind the GDI formulation.

Moisture content alone is yet not sufficient to accurately evaluate stability in the tropical atmosphere. Other processes such as the trade wind inversion (TWI) and mid-level circulations strongly modulate thermal and moisture profiles. The TWI (Riehl, 1954; Glickman, 2000) is an extensive subsidence inversion that forms in the descending branches of the Hadley circulation (Raymond 2000b) and dominates vast areas of the tropics. The TWI is typically characterized by a mild increase in temperature and a sharp decrease in moisture content from base to top, features that largely control cloud growth through stabilization and dry air entrainment. Strong inversions and/or low bases limit vertical development due to enhanced negative buoyancy and entrainment of dry air into the clouds that attempt to grow vertically. On the contrary, weak and/or elevated inversions favor vertical development and precipitation. If deep convection manages to develop through a weak or elevated inversion, it will release water vapor into the free troposphere. This 'unexpected' moistening could favor the development of new convective cells ultimately setting up of the Moisture-Convection feedback mechanism and a fair-to-stormy weather transition. Considering the characteristics of the TWI is thus essential for an accurate prediction of tropical convection. Figure 2 illustrates this, where three wet season morning soundings with different TWI features led to different afternoon convective regimes.

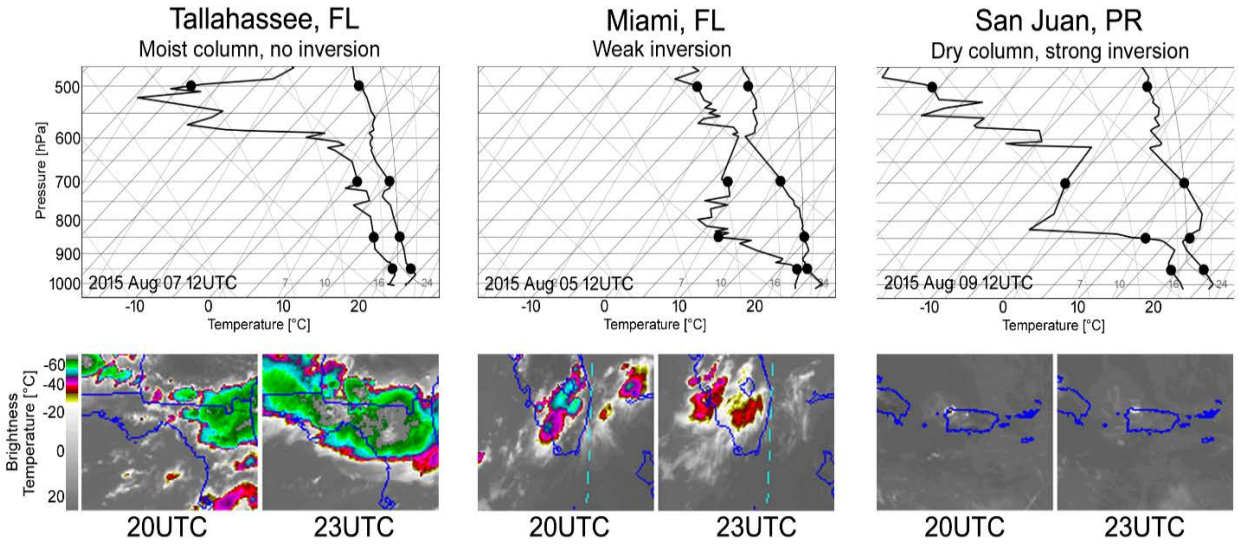

Figure 2. 12UTC soundings (top) and corresponding GOES IR4 Brightness Temperature imagery near 20 and 23UTC (bottom) to illustrate the evolution of afternoon convection near/downstream of each station in association with the morning sounding. Soundings are courtesy of the University of Wyoming (http://weather.uwyo.edu/upperair/sounding.html, 2015) and satellite images courtesy of CIRA (http://rammb.cira.colostate.edu/ramsdis/online/rmtc.asp, 2015). The GDI calculation points have been added to the soundings for later reference.

Figure 2 displays three morning soundings and corresponding afternoon GOES IR4 imagery at 20 and 23UTC to illustrate the associated evolution of convection. The Tallahassee sounding shows no inversion and a very moist column from the surface through 600hPa. This resulted in widespread thunderstorms that continued intensifying from the early afternoon (20UTC) through the late afternoon (23UTC). The San Juan sounding contrasts with the Tallahassee sounding as it shows a strong TWI near 850 hPa accompanied by very dry conditions aloft. This limited development to isolated showers. Very isolated thunderstorms were also present, but they rapidly weakened due to the entrainment of dry air when they were able to develop into the free troposphere. The Miami sounding falls in between. It shows a very weak TWI with patches of moist air aloft, especially between 650 and 550hPa. This resulted in isolated to scattered thunderstorms in the early afternoon as some of these struggled to develop through the weak inversion and marginally dry 850-700 hPa layer. The storms were already weakening by 23UTC.

Mid-level circulations also modulate the development of tropical convection. Dynamics aside, mid troughs/ridges are associated with cool/warm temperatures, which affects the stability of the underlying troposphere. Although not relevant to the calculation of stability, mid ridges and troughs also exert dynamical effects on the underlying air mass as they frequently associate with subsidence/ascent. This reflects to some extent whenever mid-level temperatures are considered in the computation of stability.

Equivalent potential temperature and tropical stability

The equivalent potential temperature EPT is the final temperature that an air parcel would attain if lifted dry adiabatically to its lifting condensation level, then pseudo-wet adiabatically to zero pressure condensing all its water vapor, and finally brought down dry adiabatically to 1000 hPa (Holton, 1972; Bolton, 1980; Bryan, 2008). EPT relates to column moisture and to the potential release of latent heat, therefore provides information about column stability in the tropics. The WPC International Desks have long relied on vertical profiles of EPT to determine the potential for moist convection in the Tropical Americas. EPT profiles not only depict warm moist unstable columns but do capture the signature of TWIs. These appear as sharp decreases of EPT with height due to the overwhelming effects of the decrease in relative humidity over the subtle increase in temperature. Figure 3 illustrates how five different convective regimes commonly encountered in trade wind environments reflect on an EPT cross section.

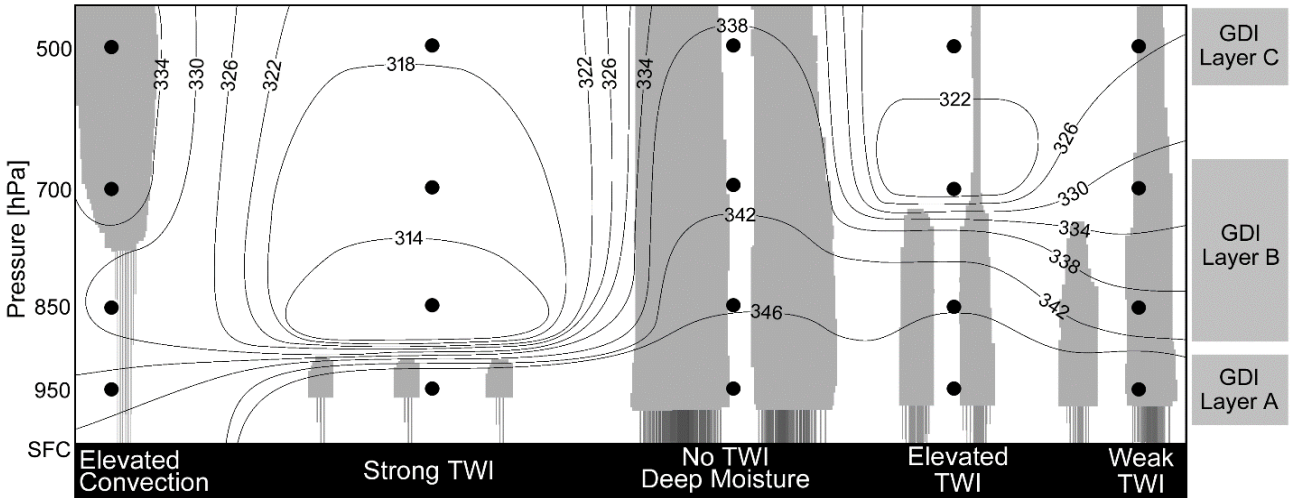

Figure 3. Schematic representation of an EPT cross section characteristic of trade wind regimes (black contours in K). Associated convection and precipitation are included. Five different convective regimes are shown, for which GDI calculation points are indicated with black circles. The three layers used for the formulation of the GDI are also included for later reference.

From the five different convective regimes described in Figure 3, it has been observed at the WPC International Desks that the one that favors the most intense convection is characterized by columns with large EPT values that decrease gently with height. This EPT distribution favors deep convective development and the potential for heavy rainfall producing thunderstorms. Conversely, the potential for thunderstorms reaches a minimum under strong TWI environmental conditions, which reflect as sharp decreases in EPT near/below 850hPa. In such environments vertical development limits to the inversion base and any precipitation is generally in the form of light rain showers. The other three scenarios fall in between. Elevated TWIs often allow sufficient development for convection to produce moderate rains. A few cells could penetrate the inversion and evolve into thunderstorms, but they are often isolated and short lived due to dry air entrainment from the free troposphere and surrounding air. A weak TWI can also favor thunderstorm development but their life span and rainfall amounts rarely exceed those of the thunderstorms that occur under the absence of a TWI. Elevated convection also occurs in the tropics, and reflects as an EPT maxima near/above 700 hPa accompanied by a relatively homogeneous profile underneath. Electrification is possible, and rainfall can be comparable to that generated under weak and elevated TWIs.

The close relationship between the vertical distribution of EPT and convection type signals the need to compute EPT as part of the GDI calculation algorithm. Calculating EPT is however non trivial. Several approaches exists, and a comprehensive summary is available on Davies-Jones (2009). EPT discrepancies produced by these different formulas are negligible in the context of weather forecasting, which motivated the selection of an expression upon simplicity. The following formula, simplified by Bolton (1980) after Betts and Dugan (1973), was selected:

$$\theta_E = \theta \exp\left(\frac{L_o r}{C_{pd} T_{LCL}}\right) \tag{2.1}$$

where L_o =2.69 × 10^6 J kg^{-1} is the latent heat of vaporization, C_{pd}=1005.7 J kg^{-1} K^{-1} is the specific heat of dry air at constant pressure, θ is the potential temperature [K], r the mixing ratio [kg kg^{-1}] and T_{LCL} the temperature at the lifted condensation level LCL [K]. The complex calculation in this formulation is the determination of T_{LCL}. Testing practices while developing the GDI revealed that replacing T_{LCL} with 850 hPa temperatures [K] produced very small differences on the final GDI values. This greatly simplifies the calculations and leads to the following expression for the calculation of EPT proxies:

$$\theta_{E\_GDI} = \theta \exp\left(\frac{L_o r}{C_{pd} T_{850}}\right) \tag{2.2}$$

3. Algorithm for the Calculation of the Gálvez-Davison Index.

The GDI is based upon thermodynamic properties of the low and mid tropical troposphere. It considers three processes that modulate tropical stability and associated convection: the availability of heat and moisture, the stabilizing/destabilizing effects of mid tropospheric ridges/troughs and the stabilizing and drying effects of the TWI. The GDI is calculated with temperatures and mixing ratios at four levels: 950, 850, 700 and 500 hPa which are used to define three layers. Layer A uses 950 hPa data and represents low tropospheric conditions. Layer B stretches from 850 hPa to 700 hPa and often captures the TWI and its characteristics. Layer C considers 500hPa data and represents the mid troposphere. The GDI was intentionally developed to produce values comparable to those of the K index for ease of comparison, which required the use of a few empirically-determined adjustment constants for its calculation.

The initial step is to compute potential temperatures θ [in K] and mixing ratios r [in kg kg^{-1}] for each layer via equations 3.1 through 3.6. Input temperatures are in [K]:

$$\theta_A = \theta_{950} = T_{950}(1000/950)^{2/7} \tag{3.1}$$

$$\theta_B = 0.5(\theta_{850}+\theta_{700}) = 0.5[T_{850}(1000/850)^{2/7}+T_{700}(1000/700)^{2/7}] \tag{3.2}$$

$$\theta_C = \theta_{500} = T_{500}(1000/950)^{2/7} \tag{3.3}$$

$$r_A = r_{950} \tag{3.4}$$

$$r_B = 0.5(r_{850}+r_{700}) \tag{3.5}$$

$$r_C = r_{500} \tag{3.6}$$

EPT proxies are then calculated for each layer by applying equation 2.2:

$$EPTP_A = \theta_A e^{(\frac{L_o r_A}{C_{pd} T_{850}})} \tag{3.7}$$

$$EPTP_B = \theta_B e^{(\frac{L_o r_B}{C_{pd} T_{850}})} + \propto \tag{3.8}$$

$$EPTP_C = \theta_C e^{(\frac{L_o r_C}{C_{pd} T_{850}})} + \propto \tag{3.9}$$

where $\propto = -10$ [K] is an empirical adjustment constant.

Once EPT proxies are available, three sub-indices are calculated to represent each of the three physical processes considered relevant to trade wind convection. The first process is the availability of heat and moisture in the column which controls buoyancy and the maintenance of convection. This is represented by a dimensionless Column Buoyancy Index CBI that exhibits large values when a warm and moist mid troposphere (layer C) is reinforced by warm and moist conditions near the surface (layer A). This suggests the potential for near-ground based convection. EPT factors are first calculated for the mid and low troposphere (ME and LE) and display positive values if their respective EPT proxies exceed $\beta = 303$ [K]:

$$ME = EPTP_C - \beta \tag{3.10}$$

$$LE = EPTP_A - \beta \tag{3.11}$$

The CBI can then calculated via (3.12):

$$CBI = \left\{ \begin{matrix} \gamma \times LE \times ME & , LE > 0 \\ 0 & , LE \leq 0 \end{matrix} \right\} \tag{3.12}$$

where $\gamma = 6.5 \times 10^{-2}$ [K^{-1}] is an empirical scaling constant. The CBI is an enhancement factor and exhibits only positive values when the low troposphere is sufficiently warm and moist. The product of LE and ME results in non-linear increases in CBI values upon increases in low or mid tropospheric EPT.

A dimensionless Mid-level Warming Index MWI is then calculated. The MWI accounts for the enhancement of mid-level stability when warm ridges develop. It is thus an inhibition index that only produces negative values upon positive departures of 500 hPa temperatures from the $\tau = 263.15$K (-10C) threshold. The MWI is also calculated using a conditional expression (3.13):

$$MWI = \left\{ \begin{matrix} \mu \times (T_{500} - \tau) & , T_{500} - \tau > 0 \\ 0 & , T_{500} - \tau \leq 0 \end{matrix} \right\} \tag{3.13}$$

where $\mu = -7$ [K^{-1}] is an empirical scaling constant that sets MWI values negative.

The third and last sub-index to compute is the Inversion Index II. The II is also an inhibition factor solely and produces negative values only. It considers two processes: stability across the inversion and dry air entrainment once convective cells penetrate it. A dimensionless Stability Factor S is calculated via a simple difference of 950hPa and 700 hPa temperatures [K] via (3.14):

$$S = \sigma \times (T_{950} - T_{700}) \tag{3.14}$$

where $\sigma = 1.5$ [K^{-1}] is an empirical scaling constant. A dimensionless Drying Factor D is then calculated based on the difference of EPT between layers A and B:

$$D = \sigma \times (EPTP_B - EPTP_A) \tag{3.15}$$

The II can be then calculated based on the combined contributions of S and D using a conditional:

$$II = \left\{ \begin{matrix} 0 & ,S + D > 0 \\ S + D & ,S + D \leq 0 \end{matrix} \right\} \tag{3.16}$$

The GDI can then be calculated by simply adding the three sub-indices:

$$GDI = ECI + MWI + II \tag{3.17}$$

Improved visualization of predictor fields' matters in weather forecasting practices as it optimizes the time required by the forecaster to draw conclusions and produce a forecast. Strictly speaking, the GDI is only applicable in terrain located below 950 hPa. Numerical model data, however, is commonly extrapolated to fill layers that in reality lie under the model surface. These values are often fictitiously high but do reflect to some extent the conditions of the local troposphere. With this in mind, a correction factor was devised to account for model-terrain induced field distortion. This factor uses model surface pressure P_{SFC} [hPa] to adjust fictitious GDI values to more reasonable ones. Tests have shown that this correction still leads to high GDI-cold cloud top correlations in mountainous regions where the GDI should be inapplicable. Correlations exceed r^2=0.5 in some cases (e.g. Mexican highlands) when data is intercompared at horizontal resolutions of 2°×2°. The dimensionless Orography Correction Factor C_O is defined by:

$$C_O = P_3 - \frac{P_2}{P_{SFC} - P_1} \tag{3.18}$$

where $P_1 = 500$ [hPa], $P_2 = 9000$ [hPa] and $P_3 = 18$ are all empirical constants adjusted to improve GFS-derived GDI visualization over elevated terrain. This leads to an alternative Orography-Corrected GDI formulation:

$$GDIc = ECI + MWI + II + C_O = GDI + C_O \tag{3.19}$$

4. GDI Skill in the Tropical Americas-Caribbean Basin: validation results.

The skill of the GDI in tropical North and South America was investigated via a simple validation process carried out during their respective 2013-14 rainy seasons. It consisted of the comparison of GFS-derived GDI values against GOES IR4 Brightness Temperatures (BT) in North America (Table 2), and against Outgoing Long Wave Radiation (OLR) in South America (Table 3).

Table 2. Data used for the validation of the GDI over tropical North America.

Intercomparison Data	Averaging Method	Original data source	Reference
Brightness Temperatures	12-hour averages (00Z-12Z) computed daily during July-October 2013	Infrared-4 satellite data from GOES13, available every 30 minutes	RAMSDIS server online at http://rammb.cira.colostate.edu/ramsdis/online/rmtc.asp
GDI	12-hour averages (00Z-12Z) computed daily from 01 Jul through 31 Oct 2013	GFS 00UTC 1° daily analyses and forecasts (00-F12) from 01 Jul through 31 Oct 2013	NCEP ftp server online at ftp://tgftp.nws.noaa.gov/ /SL.us008001/ST.opnl/

Table 3. Data used for the validation of the GDI over tropical South America.

Intercomparison Data	Averaging Method	Original data source	Reference
Outgoing Long Wave Radiation	24-hour averages (00Z-00Z) computed daily during October 2013-November 2014	24-hour averages (00Z-00Z)	NCEP ftp server online at http://www.esrl.noaa.gov/psd/data/gridded/data.interp_OLR.html (Liebmann and Smith, 1996).
GDI	24-hour averages (00Z-00Z) computed daily from 01 Oct 2013 through 28 Feb 2014	GFS 00UTC 1° daily analyses and forecasts (00-F12) from 01 Oct 2013 through 28 Feb 2014	NCEP ftp server online at ftp://tgftp.nws.noaa.gov/ /SL.us008001/ST.opnl/

Both BT and OLR capture the general structure and depth of tropical convection. Some contamination by cirrus clouds is unavoidable, especially near large thunderstorms/mesoscale convective systems and near ascending subtropical upper jets. The latter are however common during winter and transition seasons, not during the summer, which limited their impact during the validation period. The intercomparison exercise was extended into other traditional stability indices and quantities to compare their performance with that of the GDI. These quantities comprise the Lifted, Total Totals and K indices, and the CAPE, all calculated from GFS data following the method indicated in Tables 2 and 3. The data were intercompared at two different horizontal resolutions: 1° and 2°. It is natural to expect a significant increase in index skill when convection-related data is interpolated into a coarser grid. This is especially true in the case of tropical convection as it organizes into complex mesoscale structures that are often discrete within a broad region of instability. This produces a sharp decrease in correlation values as intercomparison exercises move into finer grids. An example is summarized in Figure 4, which compares BT-GDI r^2 (top) and BT-K r^2 (bottom) constructed at horizontal resolutions of 1° (left) and 2° (right), where r^2 is the determination coefficient (equation 4.1). With this in mind, the analysis will be hereafter presented at resolutions of 2° for all quantities.

The dimensionless determination coefficient r^2 represents the fraction of the variance shared by the quantities compared and is calculated via:

$$r^2 = \frac{n\sum xy - (\sum x)(\sum y)}{\sqrt{n(\sum x^2) - (\sum x)^2}\sqrt{n(\sum y^2) - (\sum y)^2}} \quad (4.1)$$

where n is the sample size, x corresponds to BT [K] for North America and OLR [W m^{-2}] for South America, and y corresponds to index values in this validation exercise.

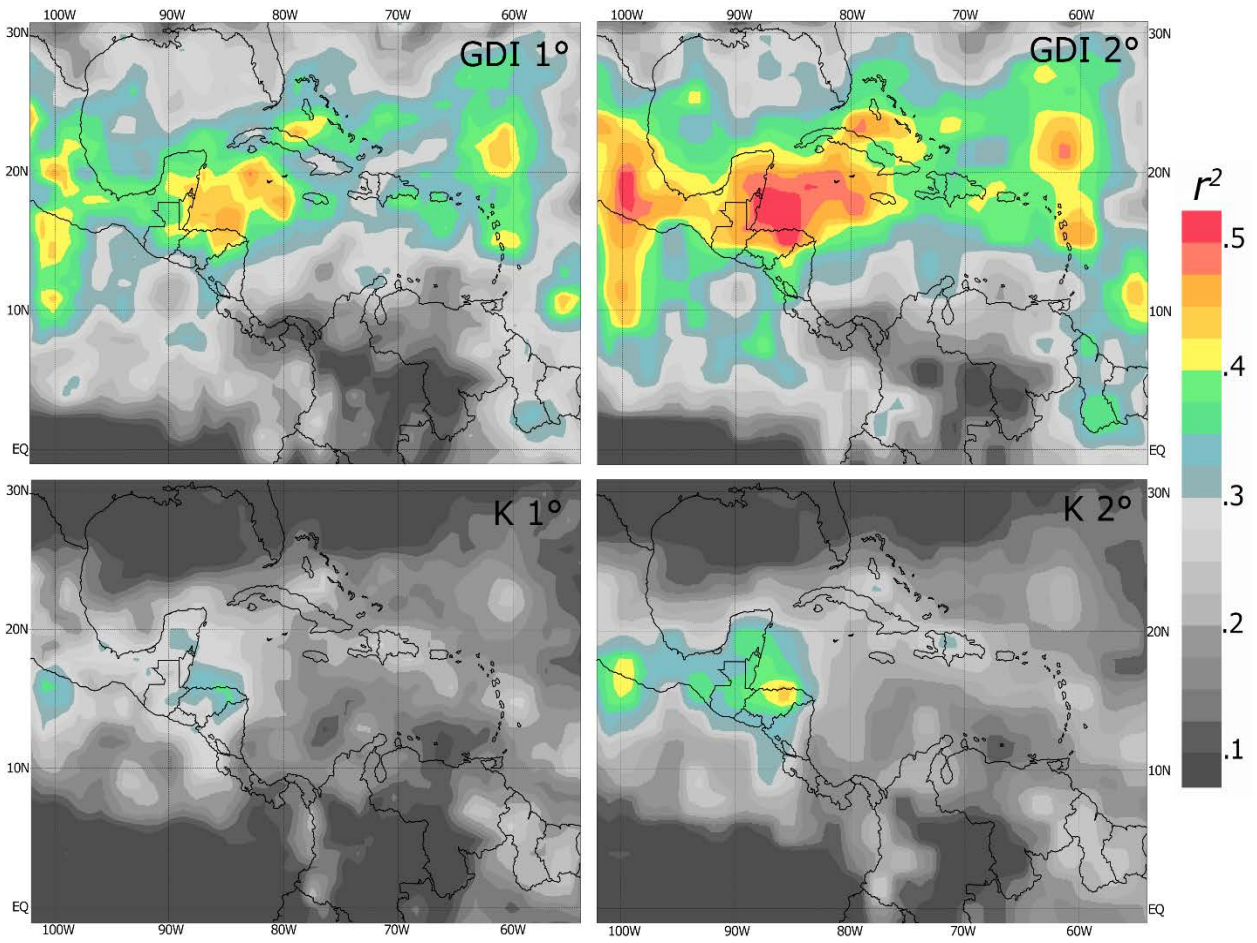

Figure 4. Example of the differences in BT-GDI (top) and BT-K (bottom) r^2 when computed at resolutions of 1° (left) versus 2° (right). The values were obtained using 12-hr averages calculated daily over parts of Tropical North America and the Caribbean during the 01 July – 31 October 2013 period.

One limitation of the current method is the conditioning of index skill to the skill of the 00-UTC GFS solutions through the first 12 and 24 forecast hours for North and South America respectively. Index skill intercomparison is however barely compromised given that index values are computed from the same data. Intercomparison is hence valid under the assumption that the model captured the tropospheric evolution reasonably well during the first hours of the forecast period. This is generally true, which is documented in verification results prepared by the Global Climate and Weather Modeling Branch of the NCEP's Environmental Modeling Center (http://www.emc.ncep.noaa.gov/GFS/perf.php)

Results

The results are encouraging as they show that the GDI outperforms most stability indices on the depiction of tropical convection. This is exemplified in Figure 5, which shows a comparison of r^2 calculated for the five stability indices/quantities tested over the 01 July – 31 October 2013 period.

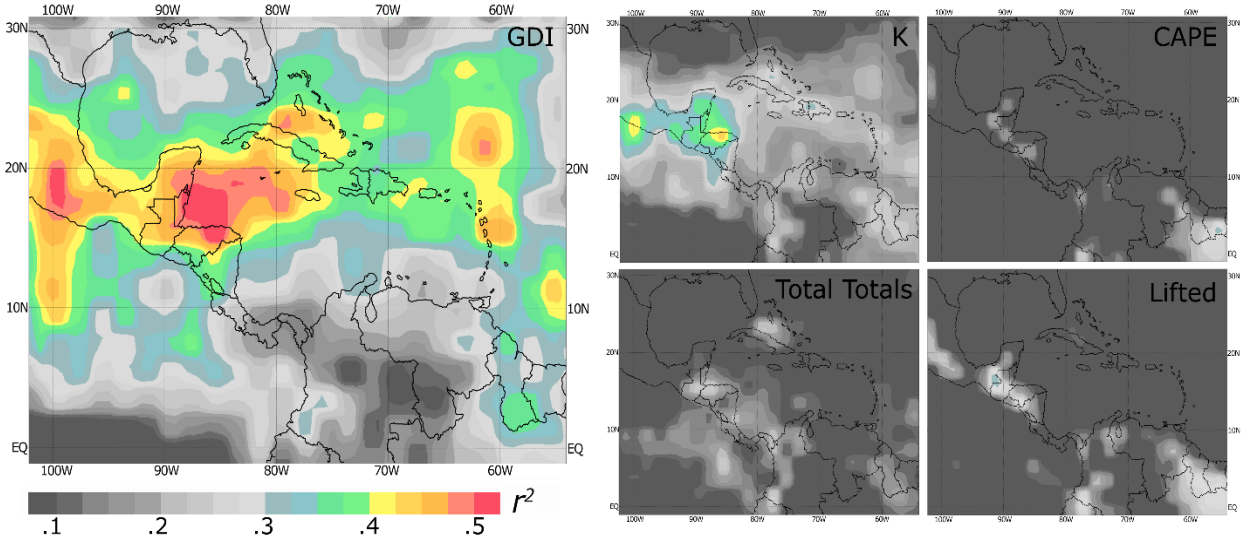

Figure 5. Determination coefficient r^2 for BT against the GDI (left), K (top center), CAPE (top right), Total Totals (bottom center) and Lifted (bottom right) computed over tropical North America and the Caribbean during the 01 July – 31 October 2013 period.

Figure 5 shows that the largest index-BT correlations for a given point in the domain where largely attained by the GDI among all indices compared. The largest correlations were attained over the 15N-25N belt that stretches from the central Caribbean/Nicaragua north into most of Mexico and the Florida peninsula. This includes the Bahamas, Leeward Islands and the Greater Antilles where the GDI was able to explain over 35% of BT variances alone. The skill is particularly remarkable in the Gulf of Honduras/Yucatan Peninsula and in central Mexico where the GDI resolves over 45% of BT variances. The high correlations encountered in Mexico are particularly noteworthy given that most of the terrain lies over 950 hPa. This is an encouraging result given that central Mexico is a largely populated region that includes Mexico City, an urban area that comprises near 20 million people.

Simple differences of GDI r^2 values minus those of the other indices/quantities is presented in Figure 6 using a resolution of 2°. The plots shows how the GDI outperforms all indices and only competes with the K index in areas close to the ITCZ and the Panamanian Low. The increased skill over latitudes to the north of 16N-18N is remarkable as the GDI explains over 15% more of BT variance than the K. This improved skill peaks over the Gulf of Mexico/Florida and Cuba/Jamaica where GDI outperforms the K by resolving an additional 20-30% of the BT variance.

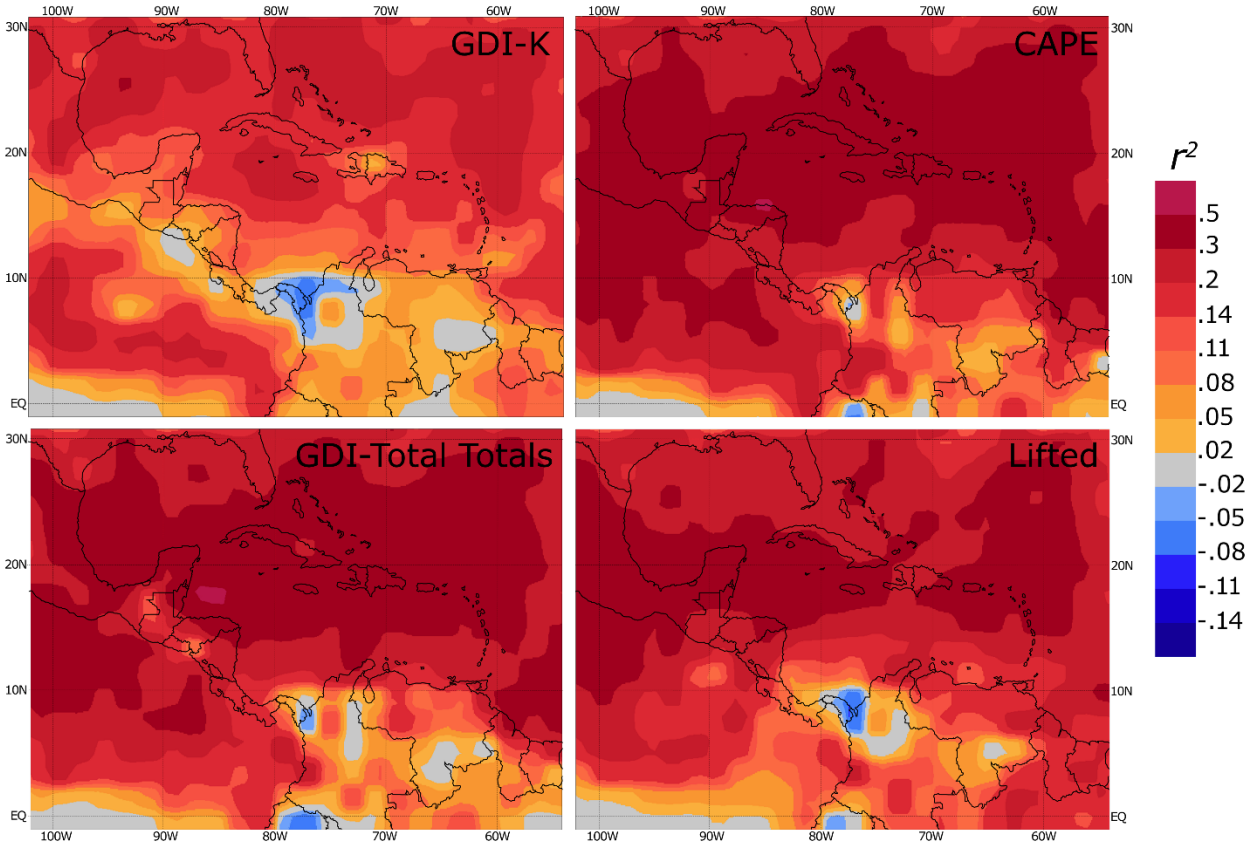

Figure 6. Differences between the GDI-r^2 minus that of the K (a), CAPE (b), Total Totals (c) and Lifted (d) computed over tropical North America and the Caribbean Basin during the 01 July – 31 October 2013 period.

A similar analysis was conducted over South America following the method described in Table 3 and is presented in Figure 7. Index-OLR r^2 values were calculated for the GDI, Lifted, K and Total-Totals. The results are encouraging as well, with the GDI also outperforming traditional stability indices over most of the domain when comparing at horizontal resolutions of 2°. The GDI was also able to resolve over 45% over vast areas especially eastern Brazil and Venezuela which are dominated by trade wind regimes. Correlations in these regions are larger than those found in North America as r^2 exceeds 70% in parts of the states of Minas Gerais and Espirito Santo in southeastern Brazil. In densely populated areas such as Sao Paulo and Rio de Janeiro the GDI outperformed all indices tested and resolved 55-65% of the OLR variance. Although the comparison was made in terms of OLR instead of BT, correlation values were much larger over northern Venezuela than those found in the North America/Caribbean analysis (Figure 4). This suggests that the GDI skill increases during the transition to/arrival into the Northern Hemisphere dry season. This is expected due to an increased influence of trade wind inversions into the variability of convection for which the GDI has been explicitly developed. Conversely, subsidence inversions and mid tropospheric thermal variations are often limited during the rainy season in the deep tropics. This is the case of northern Venezuela/Colombia/Panama during July-October (Figure 4). This is also the case in the central and western Amazon basin (western Brazil, eastern Peru) where rainy season air masses have lost their trade-wind thermodynamic characteristics once they arrive from the east after interacting with most of Tropical South America, which results in a decrease of index skill.

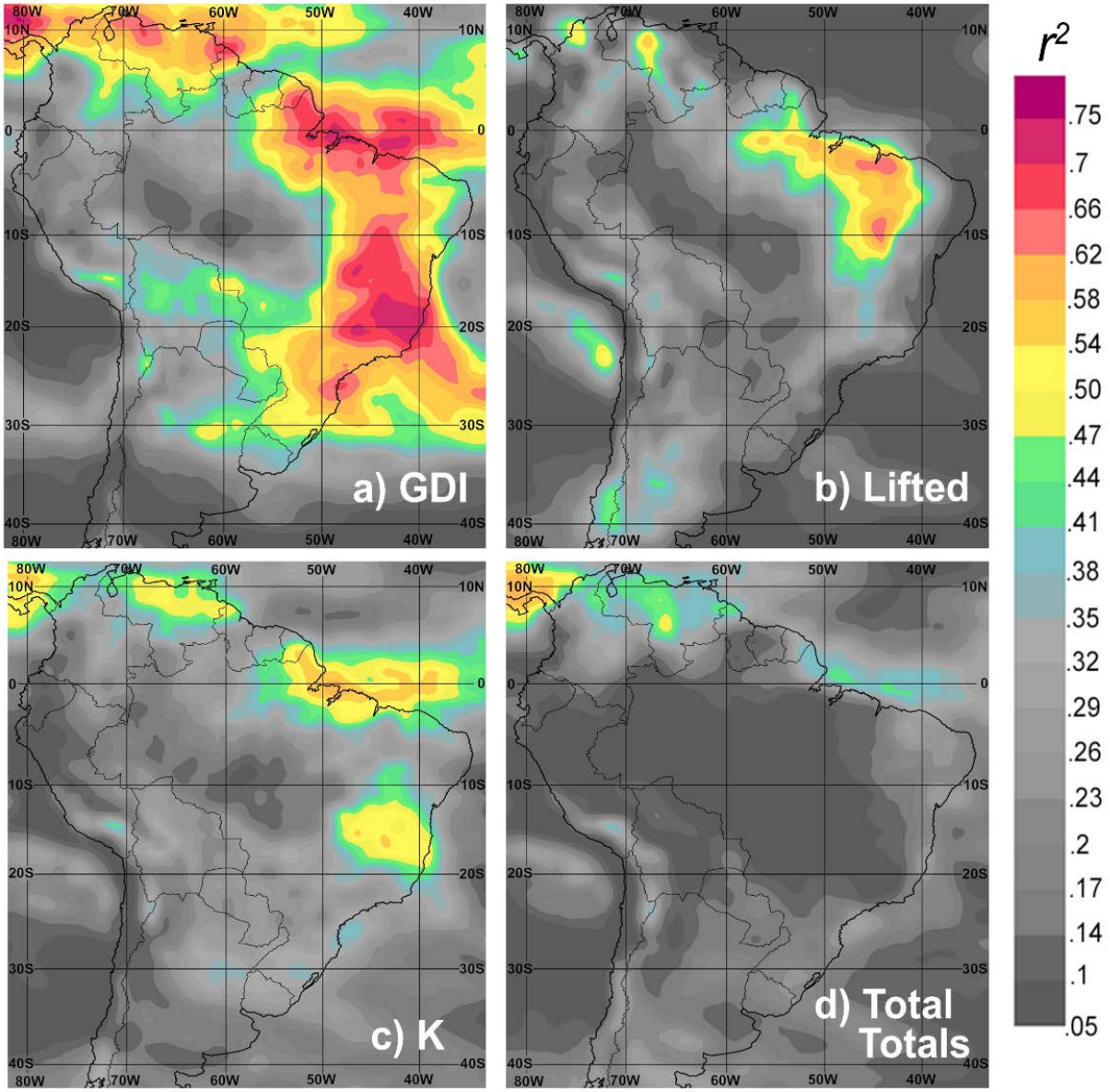

Figure 7. Determination coefficient r^2 for BT against the GDI (a), Lifted (b), K (c) and Total Totals (d) computed over tropical South America during the 01 October 2013 – 28 February 2014 period.

Similar to Figure 6, Figure 8 shows simple differences calculated of GDI r^2 values minus r^2 of the other indices tested. Once again the results show that the GDI outperformed some of the traditional stability indices over most of the domain. Figure 8 also shows how other indices, especially the Lifted and Total Totals outperform the GDI in extra tropical locations that stretch south of a line from Central Chile into extreme northern Patagonia/southern Buenos Aires province in Argentina, an expected result due to the GDI dependence on deeper tropical/subtropical moisture. GDI skill is also limited over the cold current stratocumulus regime off the coasts of northern Chile and southern Peru. But this is explicable as the thermal structure of this regime is much cooler than other trade wind regimes and associated inversions are regularly found below 950 hPa differing from those encountered in warmer trade wind environments.

Elsewhere in South America the GDI outperforms most indices including the K. The skill increase over the K is particularly remarkable over most of eastern Brazil where the GDI resolves an additional 15-30% of the OLR variance than the K. The enhanced skill extends west into Paraguay/Bolivia and southern

Peru, where the GDI explains an additional 10-20% of the variance resolved by the K. The most remarkable skill improvement coincides with densely populated regions of southeastern Brazil across the states of Parana, Sao Paulo, Minas Gerais, Rio de Janeiro and Espirito Santo where the GDI explains over 30% of the amount of OLR variance resolved by the K.

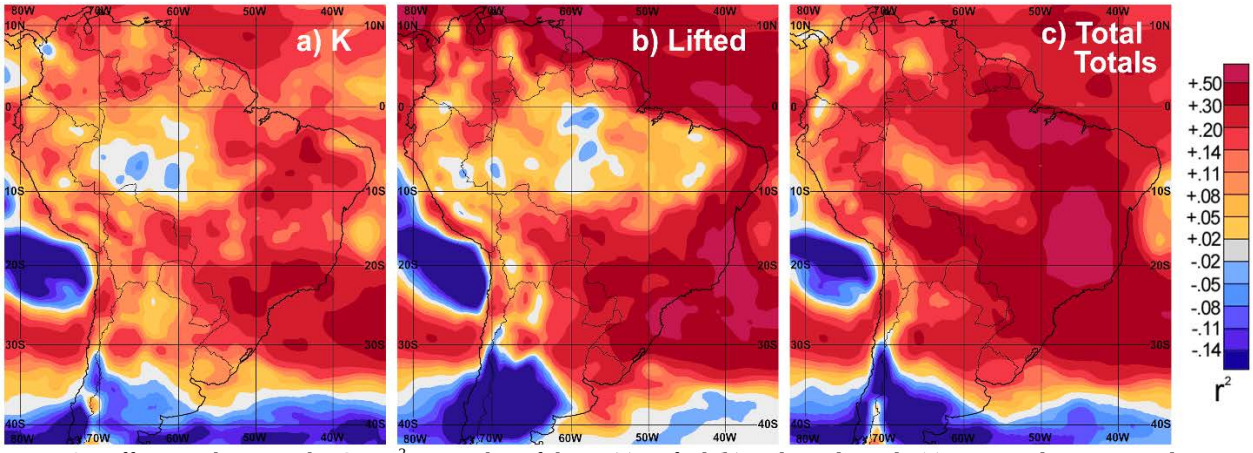

Figure 8. Differences between the GDI-r^2 minus that of the K (a), Lifted (b) and Total Totals (c) computed over tropical South America during the 01 October 2013 – 28 February 2014 period.

The GDI excels in tropical regions, especially in trade wind regimes. But validation results also show that it can be used in extra tropical locations during the summer. In this case it is essential to use the GDI in combination with other stability indices and dynamical fields in order to assess the potential for convection. Validation results suggest that the areas of strongest convection in extra tropical locations such as northern Argentina/Uruguay/Paraguay/southern Brazil or the eastern United States occur often downwind from GDI maxima and/or between the GDI maxima and the region of the strongest dynamical forcing.

Determination of expected convection types from GDI values

Expected convection types can be determined via the generation of tables from scatterplots that relate GDI values to cold cloud temperatures. Although low GDI values associate with strong subsidence inversions/dry air masses and a low potential for thunderstorms, and vice versa; the exact nature of the GDI-cold cloud relationship varies upon region and season, to a lesser extent. An example is presented in Figure 9.

Figure 9 illustrates an example where OLR-GDI scatterplots were used to construct GDI-convective regime tables for two contrasting locations in South America. Note that the distributions vary for each location. The large correlations/limited scattered in Minas Gerais (top) result on higher confidence GDI-Convective Regime tables. In contrast, limited correlations over the Altiplano/Bolivian High Plains lead to more uncertainty. The color coding illustrates seasonality effects on index skill. In the Altiplano, for example, dry season convection (browns for October-November) produced a wide scatter that suggests limited GDI skill during this period. A more linear distribution of greens (January-February) suggest a significant increase on the skill during the wet season, partly tied the seasonal increase in column moisture content.

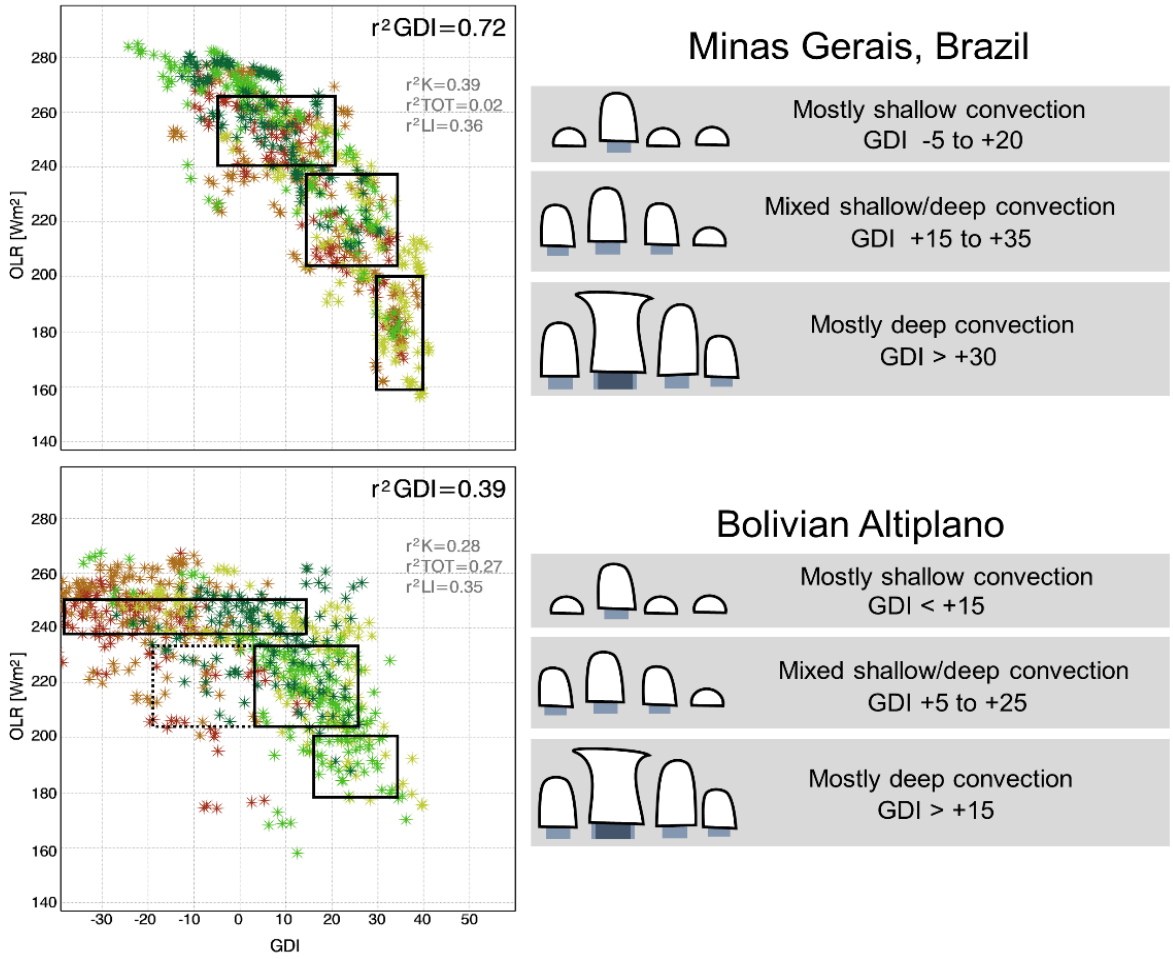

Figure 9. OLR-GDI scatterplots that illustrate a simple method to determine the expected convective regime from GDI value ranges per location. Examples are provided for two different regions in South America that produced different correlations and scatter distributions: Minas Gerais in southeastern Brazil (areal averages over 47W-42W, 22S-17S) and the Bolivian Altiplano (areal averages over 70W-65W, 22S-17S). Scatter colors range from deep brown through yellow to green for each month during the rainy season starting in October 2013 and ending in February 2014.

Aside from recommended local and seasonal adjustments, the data collected during the validation permitted the construction of a general GDI-Convective Regime table that can be used as a support tool during the process of forecasting the risk for thunderstorms and rain showers (Table 4). It should be noted that table 4 considers potential response of convection to the convective instability resolved by the GDI alone. Other factors such as dynamically-driven ascent/descent can enhance or decrease the potential for the described types of convection.

Table 4. General GDI-Convection type table constructed upon validation results.

GDI Value	Expected Convective Regime
>+45	Scattered to widespread thunderstorms likely. Locally heavy rains likely.
+35 to +45	Scattered thunderstorms and/or scattered to widespread rain showers. Locally heavy rains possible.
+25 to +35	Isolated to scattered thunderstorms and/or scattered showers. Locally heavy rains possible.
+15 to +25	Isolated thunderstorms and/or isolated to scattered showers.
+05 to +10	Isolated to scattered showers. If a thunderstorm develops will be brief and very isolated.
<+5	Strong TWI likely. Any rain showers that develop will produce light rain.

Applications

As a stability index, the GDI has demonstrated skills that are highly applicable to meteorologists that specialize in the forecast of thunderstorms and other types of moist convection. This includes specialties such as those dealing with general/public forecasts, quantitative precipitation forecasts and operational support to civil aviation to name a few. In support of civil aviation, the GDI has proved to be a useful tool for the planning and adjustment of flight routes. Since 2014, the GDI has been heavily used in support of aviation operations by the Federal Aviation Administration - Air Traffic Control System Command Center in Warrenton, Virginia (Mike Eckert and Joe Carr, FAA, personal communication, 2014); and in 2015 this extended into CWSU Met at ZJX (Jacksonville, FL) with successful results and comments on how the GDI excels particularly under rich westerly flow (Mike Eckert and Joe Carr, FAA, personal communication, 2015).

Internationally, many national meteorological centers in the Americas and across the Caribbean have used the GDI since 2014 for the prediction of convection type and for the generation of quantitative precipitation forecasts with excellent results. Some use the GFS-derived index input made available on the WPC International Desks website (http://www.wpc.ncep.noaa.gov/international/gdi/), while others have opted to locally generate the forecast. In some instances the GDI has been implemented into mesoscale models as it is the case of the Uruguay Weather Service, the Instituto Uruguayo de Meteorología, where a 10km resolution WRF derived GDI is used to generate operational weather forecasts and is available online at http://www.meteorologia.com.uy/modelos/prediccionNumerica. This is also the case of El Salvador's Ministerio del Medio Ambiente y Recursos Naturales where the GDI is computed routinely from 30km, 15km and 5km WRF model output and is available at http://modelacionnumerica.tk/. Countries that use the GDI routinely in weather forecasting practices include the United States, Mexico, Honduras, El Salvador, Colombia, Costa Rica, Cuba, the Dominican Republic, Suriname, Trinidad and Tobago, Peru, Uruguay and Chile (personal communication, 2015).

The GDI has also excelled as a tool for the detection and prediction of tropical waves in the easterly trades and for the analysis and position of the intertropical convergence zone, as it resolves finer convectively unstable structures in the tropical atmosphere that other indices are unable to resolve to the same degree. This is of particular use for the Caribbean Basin/Mexico and the southeastern United States, where waves in the trades play an important role in the generation of summer convection and rainfall. An example is provided in Figure 10, where GFS-derived GDI is used to highlight the instability associated with perturbations in the easterly trades in combination with 850-700 hPa average streamlines. Figure 10 shows the west-northwestward progression of four waves in the trades and associated regions of convective instability. The waves are denoted with solid black lines and labeled with letters A, B, C and D for position identification. The vorticity at 500 hPa is also included to identify Tropical Upper Tropospheric Troughs (TUTT), a recurrent feature in subtropical summer convection. The GDI captures well the instability associated with the TUTT by the consideration of mid-level temperatures. In Figure 10, an L is used to denote a TUTT low that meanders from just east of the Central Bahamas into southeastern Florida from July 7th to the 9th while interacting with a wave in the trades.

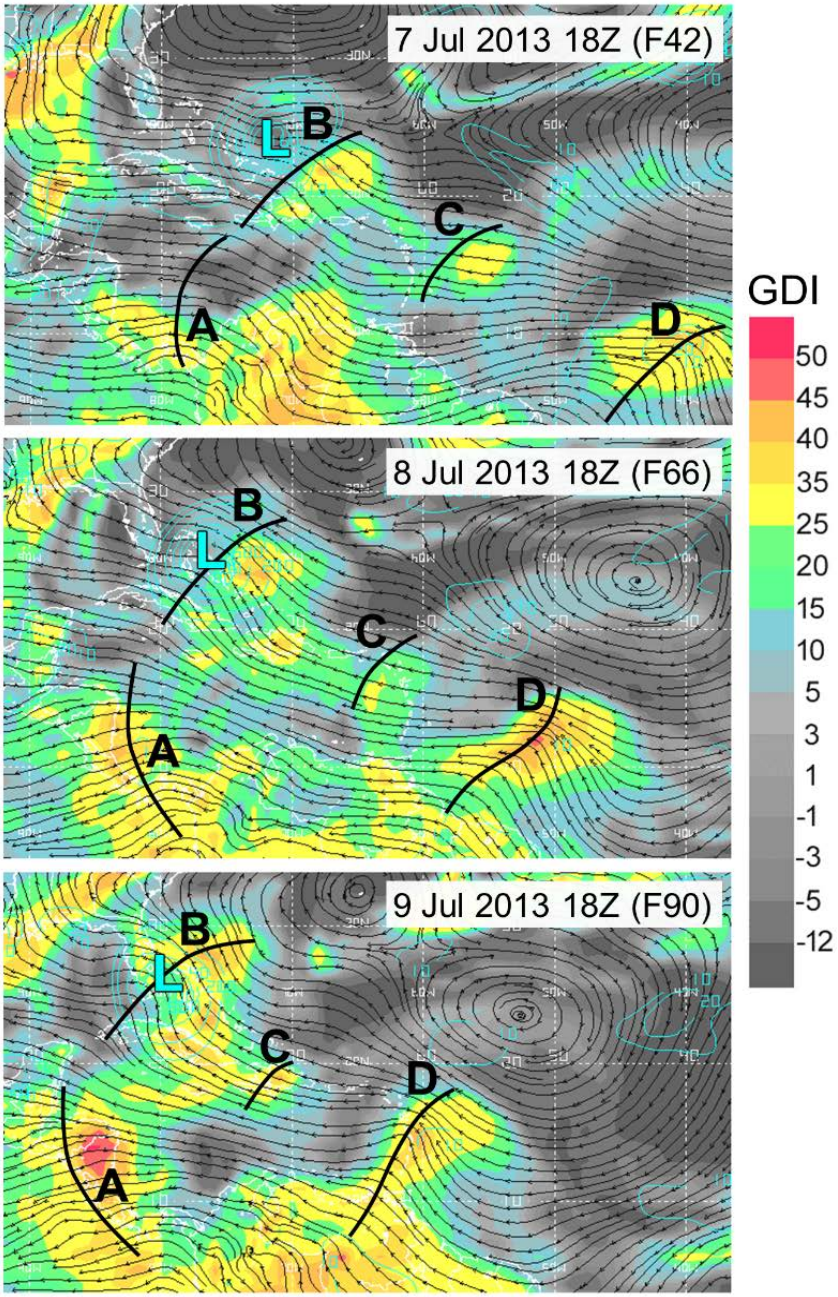

Figure 10. Three-day evolution of the GDI (shaded), 700-850 hPa streamlines (black) and 500 hPa vorticity × $10^{-6}s^{-1}$ (light blue contours) in GFS model forecast data F42, F66, F90 showing the west-northwestward progression of waves in the trades.

Excessive values in the vicinity of thermal lows

As noted, the GDI highly relies on EPT which is related to the amount of moisture and heat in the troposphere. Although this is tightly related to tropical instability, EPT can become excessively high in lower tropospheric regions near thermal lows. Temperatures become excessively warm in these regions and their contribution into the calculation of EPT highly overwhelms that of moisture. This sets off the balance between moisture and heat that relates otherwise well with tropical convection, and the GDI should be used with caution in these regions. Future work includes the development of an adjustment factor to enhance GDI skill in the vicinity of thermal lows.

5. Summary and Conclusions.

The Gálvez-Davison Index GDI was developed to improve the detection and accurate forecast of tropical convective instability with emphasis on trade wind regime convection, motivated by the limited skill of traditional stability indices used for the forecasting of such. It consists of the algebraic sum of three dimensionless sub-indices. These describe the column availability of heat and moisture, the stabilizing/destabilizing effects of warm mid ridges/cool mid troughs, and the stabilizing and drying effects of trade wind-type inversions.

Validation of the index over the Caribbean and tropical/subtropical North and South America during their corresponding 2013-14 warm/rainy seasons shows that the GDI outperforms most traditional indices on the detection of the potential for the development of cold clouds often associated with tropical convection. This is true even when compared with the K index, so far the index of choice to forecast the potential for tropical and air mass thunderstorms in the Americas. Intercomparison results attained at horizontal resolutions of 2° show that the GDI outperforms the K over more than 90% of a domain that stretches from the southern United States to central Argentina and Chile. The GDI particularly excels in 15°-25° latitude belts and particularly in the eastern side of continents where trade wind type convection dominates. In these regions, it resolves an additional 15-30% of cold cloud variances that the K. This is especially remarkable over densely populated areas such as Mexico City and Sao Paulo/Rio de Janeiro where it outperforms the K by resolving near or more than 30% additional variance becoming the most skillful of the stability indices evaluated for thunderstorms forecasting.

In terms of resolving cold cloud variance itself, the GDI skill peaks across Jamaica/Cuba/Gulf of Honduras/Yucatan west into southern and central Mexico where it resolves over 45% of the variance of cold clouds. In South America it resolves over 50% of cold cloud variance in most of Eastern Brazil, peaking at near 75% over Minas Gerais and Espirito Santo. It is also skillful along the southeastern United States, Gulf of Mexico and Florida where it resolves as much as 25-40% of cold cloud variance, which exceeds the skill of all the tested indices and outperforms that of the K by 20-30%. This is of great use for summer convection forecasting in Florida and adjacent portions of the Southeastern United States, where activities are frequently affected by the development of diurnal thunderstorms.

The GDI also excels as a tool for the detection of bands of enhanced convective instability associated with the ITCZ and waves in the trades. This is of great use for forecasting trade wind wave positions and associated convective instability, which play a dominant role on summer/rainy season convection in the Caribbean, Central America, Mexico and the southeastern United States.

Experimental versions of the GDI have already been implemented in several weather services across the Americas and is being used routinely used for the prediction of thunderstorms with applications on precipitation forecasting and aviation among others. Future work includes more thorough validation exercises using lag correlations, the determination of skill tables tailored for specific locations, and the device of an optional correction that improves GDI skill under thermal low and other high surface temperature environments.

References

Betts, A. K., and F. J. Dugan, 1973: Empirical formula for saturation pseudo-adiabats and saturation equivalent potential temperature. J. Appl. Meteor., 12, 731–732.

Blanchard, D. O, 1998: Assessing the vertical distribution of Convective Available Potential Energy. Weather and Forecasting, 13, 870-877.

Bolton, D, 1980: The computation of equivalent potential temperature. Monthly Weather Review, 108, 1046-1053.

Bryan, G. H., 2008: On the computation of pseudoadiabatic entropy and equivalent potential temperature. Monthly Weather Review, 136, 5239-5245.

Caesar, K. L. 2005: Summary of the Weather during the RICO project. NCAR/Caribbean Institute for Meteorology and Hydrology.

Davies-Jones R., 2009: On formulas for equivalent potential temperature. Monthly Weather Review, 137, 3137-3148.

Doswell, C. A. and E. Rasmussen, 1994: The effect of neglecting the virtual temperature correction on CAPE calculations. Weather and Forecasting, 9, 625-629.

Finch Z. O. and R. H. Johnson, 2010: Observational analysis of an upper-level inverted trough during the 2004 North American Monsoon Experiment. Monthly Weather Review, 138, 3540-3555.

Galway, J. G., 1956: The lifted index as a predictor for latent instability. Bull. Amer. Meteor. Soc., 528-529.

George, J. J., 1960: Weather Forecasting for Aeronautics, Academic Press, 673 pp.

Glickman, T. S., 2000: Glossary of Meteorology. Second Edition. American Meteorological Society, Boston, MA, 855pp.

Grabowski, W. W. and M.W. Moncrieff, 2004: Moisture-convection feedback in the tropics. Quart. J. Roy. Meteorol. Soc., 130, 3081–3104.

Haklander A. J., and A. Van Delden, 2003: Thunderstorm predictors and their forecast skill for the Netherlands. Atmospheric Research, 67-78, 273-299.

Holton, J.R., 1972. An Introduction to Dynamical Meteorology. Academic Press, 319 pp.

Huntrieser, H., Schiesser, H.H., Schmid, W., Waldvogel, A., 1997. Comparison of traditional and newly developed thunderstorm indices for Switzerland. Weather Forecast. 12, 108–125.

Jacovides, C.P., Yonetani, T., 1990. An evaluation of stability indices for thunderstorm prediction in Greater Cyprus. Weather Forecast. 5, 559–569.

Liebmann B. and C.A. Smith, 1996: Description of a Complete (Interpolated) Outgoing Longwave Radiation Dataset. Bulletin of the American Meteorological Society, 77, 1275-1277.

Miller, R. C., 1967: Notes on analysis and severe storm forecasting procedures of the Military Weather Warning Center. Tech. Rept. 200(R), Headquarters, Air Weather Service, USAF, 94 pp. [Headquarters, AWS, Scott AFB, IL 62225]

Miller, R. C., 1972: Notes on analysis and severe storm forecasting procedures of the Air Force Global Weather Central. Tech. Rept. 200(R), Headquarters, Air Weather Service, USAF, 102 pp. . [Headquarters, AWS, Scott AFB, IL 62225]

Moncrieff, M. and Miller, M., 1976: The dynamics and simulation of tropical cumulonimbus and squall lines, Quart. J. Roy. Meteorol. Soc., 102, 373–394.

Neelin, J. D. and I. M. Held, 1987: Modeling tropical convergence based on the moist static energy budget. Mon. Weather Rev., 115, 3–12.

Newman A., and R. H. Johnson, 2012: Mechanisms for precipitation enhancement in a North American Monsoon Upper-Tropospheric Trough. Journal of the Atmospheric Sciences, 69, 1775-1792.

Peppler, R.A., Lamb, P.J., 1989. Tropospheric static stability and central North American growing season rainfall. Mon. Weather Rev. 117, 1156–1180.

Randall D. A. and G. J. Huffman, 1980: A stochastic model of cumulus clumping. Journal of the Atmospheric Sciences, 37, pp. 2068-2078.

Raymond D. J., 2000a: Thermodynamic control of tropical rainfall. Q. J. R. Meteorol. Soc., 126, pp. 889-898.

Raymond D. J., 2000b: The Hadley Circulation as a Radiative-Convective Instability. Journal of the Atmospheric Sciences, 57, 1286-1297.

Raymond D. J. and X. Zeng, 2005: Modelling tropical atmospheric convection in the context of the weak temperature gradient approximation. Q. J. R. Meteorol. Soc., 131, pp. 1301–20.

Riehl, H., 1954: Tropical Meteorology. McGraw-Hill, New York-London, 1954. 392 pp.

Schultz, P., 1989. Relationships of several stability indices to convective weather events in northeast Colorado. Weather Forecast. 4, 73–80.

Showalter A. K., 1947: A stability index for forecasting thunderstorms. Bull. Amer. Meteor. Soc., 34, 250-252.